PROCEEDINGS OF SCIENCE

Operational experience and commissioning of the Belle II vertex detector

B. Schwenker*[g], F. Abudinén[n], K. Ackermann[n], P. Ahlburg[e], H. Aihara[ac], M. Albalawi[n], O. Alonso[ai], L. Andricek[o], R. Ayad[ah], T. Aziz[u], V. Babu[h], S. Bacher[ag], S. Bahinipati[p], Y. Bai[m], E. Barberio[a], Ti. Baroncelli[a], To. Baroncelli[a], A. K. Basith[q], G. Batignani[v,w], A. Bauer[b], P. K. Behera[q], V. Bertacchi[v,w], S. Bettarini[v,w], B. Bhuyan[r], T. Bilka[d], R. Blanco[j], F. Bosi[w], M. Boronat[a k], L. Bosisio[x,y], A. Bozek[ag], F. Buchsteiner[b], C. Camien[h], A. Caldwell[n], G. Caria[a], G. Casarosa[v,w], M. Ceccanti[w], D. Červenkov[d], V. Chekelian[n], T. Czank[ab], N. Dash[p], M. De Nuccio[v,w], B. Deschamps[e], A. Dieguez[ai], J. Dingfelder[e], Z. Doležal[d], D. Esperante[ak], P. Fischer[i], F. Forti[v,w], M. Fras[n], A. Frey[g], M. Friedl[b], J. Fuster[ak], M. Gabriel[n], K. Gadow[h], U. Gebauer[g], L. Germic[e], T. Gessler[f], D. Getzkow[f], L. Gioi[n], B. Gobbo[y], P. Gomis[ak], J. A. M. Grimaldo[ac], K. Hara[ad], M. Heck[j], T. Hemperek[e], M. Hensel[o], T. Higuchi[z], M. Hoek[k], C. Irmler[b], A. Ishikawa[ab], I. Jaegle[al],H. B. Jeon[ae], C. Joo[z], M. Kaleta[ag], J. Kandra[d], N. Kambara[ad], K. H. Kang[ae], P. Kapusta[ag], C. Kiesling[n], B. Kisielewski[ag], D. Kittlinger[n], D. Klose[o], P. Kodyš[d], C. Koffmane[o], T. Kohriki[ad], S. Koike[C,ad], I. Komarov[y], I. Konorov[m], S. Krivokuca[o], H. Krüger[e], T. Kuhr[l], W. Kühn[f], M. Kumar[s], R. Kumar[t], P. Kvasnička[d], C. La Licata[x,y], C. Lacasta[ak], K. Lalwani[s], L. Lanceri[x,y], J. S. Lange[f], K. Lautenbach[f], J. Y. Lee[a f], S. C. Lee[ae], U. Leis[n], P. Leitl[n], D. Levit[m], Y. Li[an], J. Libby[q], G. Liemann[o], Z. Liu[c], T. Lueck[v,w], F. Lütticke[e], L. Macharski[h], P. Mammini[w], C. Mariñas[e], A. Martini[v,w], S. N. Mayekar[u], S. Mccarney[n], G. B. Mohanty[u], T. Morii[z], H. G. Moser[n], D. Moya[a j], F. J. Mueller[h], F. Müller[n], D. Münchow[f], K. R. Nakamura[ad], H. Nakayama[ad] ,Z. Natkaniec[ag], C. Niebuhr[h], J. Ninkovic[o], Y. Onuki[ac], W. Ostrowicz[ag], U. Packheiser[h], A. Paladino[z], E. Paoloni[v,w], H. Park[ae], B. Paschen[e], S. Paul[m], I. Peric[j], F. Poblotzki[h], K. Prasanth[u], A. Profeti[w], A. Rabusov[m], I. Rashevskaya[A,y], K. K. Rao[u], S. P. Reiter[f], Resmi P. K.[q], R. Richter[o], M. Ritter[l], M. Ritzert[i], G. Rizzo[v,w], M. Rozanska[ag], S. Rummel[l], D. Sahoo[u], J. G. Sanchez[a j], L. Santelj[am], J. Sasaki[ac], N. Sato[ad], B. Scavino[k], G. Schaller[o], M. Schnecke[o], F. Schopper[o], H. Schreeck[g], S. Schultschik[b], C. Schwanda[b], R. Sedlmeyer[n], C. Sfienti[k], F. Simon[n], S. Skambraks[n], Y. Soloviev[h], B. Spruck[k], R. Stever[h], U. Stolzenberg[g], J. Stypula[ag], J. Suzuki[ad], E. Tafelmayer[o], M. Takahashi[h], S. Tanaka[ad], H. Tanigawa[ac], G. N. Taylor[a], R. Thalmeier[b], T. Tsuboyama[ad], P. Urquijo[a], I. Vila[a j], A. L. Virto[a j], L. Vitale[x,y], S. Vogt[n], M. Vos[ak], K. Wan[ac], C. Wang[c], S. Watanuki[ab], M. Watanabe[C,aa], I. J. Watson[ac], J. Webb[a], N. Wermes[e], C. Wessel[e], J. Wiechczynski[ag], P. Wieduwilt[g], S. Williams[a], H. Windel[n], H. Ye[h], H. Yin[b], L. Zani[v,w], J. Zhao[c]

PoS(VERTEX2018)006

(Belle II DEPFET, PXD, and SVD Collaborations)
[a] *School of Physics, University of Melbourne, Melbourne, Victoria 3010, Australia*
[b] *Institute of High Energy Physics, Austrian Academy of Sciences, 1050 Vienna, Austria*
[c] *Institute of High Energy Physics, CAS, 19B Yuquan Road, Shijingshan District, Beijing, China*
[d] *Faculty of Mathematics and Physics, Charles University, 121 16 Prague, Czech Republic*
[e] *University of Bonn, 53115 Bonn, Germany*
[f] *Justus-Liebig-Universität Gießen, 35392 Gießen, Germany*
[g] *II. Physikalisches Institut, Georg-August-Universität Göttingen, 37073 Göttingen, Germany*
[h] *Deutsches Elektronen–Synchrotron, 22607 Hamburg, Germany*
[i] *Institute for Computer Engineering, Heidelberg University, 69117 Heidelberg, Germany*
[j] *Karlsruhe Institute of Technology, Hermann-von-Helmholtz-Platz 1, 76344 Eggenstein-Leopoldshafen, Karlsruhe, Germany*
[k] *Johannes Gutenberg University Mainz, 55099 Mainz, Germany*
[l] *Ludwig Maximilians University, 80539 Munich, Germany*
[m] *Technical University of Munich, Arcisstrasse 21, D-80333 Munich, Germany*
[n] *Max Planck Institute for Physics, D-80805 Munich, Germany*
[o] *Halbleiterlabor der Max-Planck-Gesellschaft, Otto-Hahn-Ring 6, D-81739 Munich, Germany*
[p] *Indian Institute of Technology Bhubaneswar, Satya Nagar, India*
[q] *Indian Institute of Technology Madras, Chennai 600036, India*
[r] *Indian Institute of Technology Guwahati, Assam 781039, India*
[s] *Malaviya National Institute of Technology Jaipur, Jaipur 302017, India*
[t] *Punjab Agricultural University, Ludhiana 141004, India*
[u] *Tata Institute of Fundamental Research, Mumbai 400005, India*
[v] *Dipartimento di Fisica, Università di Pisa, I-56127 Pisa, Italy*
[w] *INFN Sezione di Pisa, I-56127 Pisa, Italy*
[x] *Dipartimento di Fisica, Università di Trieste, I-34127 Trieste, Italy*
[y] *INFN Sezione di Trieste, I-34127 Trieste, Italy,* [A] *presently at TIFPA - INFN, I-38123 Trento, Italy*
[z] *Kavli Institute for the Physics and Mathematics of the Universe (WPI), University of Tokyo, Kashiwa 277-8583, Japan*
[aa] *Department of Physics, Niigata University, Niigata 950-2181, Japan,* [B] *presently at Nippon Dental University, Niigata 951-8580, Japan*
[ab] *Department of Physics, Tohoku University, Sendai 980-8578, Japan*
[ac] *Department of Physics, University of Tokyo, Tokyo 113-0033, Japan*
[ad] *High Energy Accelerator Research Organization (KEK), Tsukuba 305-0801, Japan,* [C] *deceased*
[ae] *Department of Physics, Kyungpook National University, Daegu 702-701, Korea*[af] *Department of Physics and Astronomy, Seoul National University, Seoul 151-742, Korea*
[ag] *H. Niewodniczanski Institute of Nuclear Physics, Krakow 31-342, Poland*
[ah] *Department of Physics, Faculty of Science, University of Tabuk, Tabuk 71451, Saudi Arabia*
[ai] *University of Barcelona, C/Marti Franques, 1., 08028-Barcelona, Spain*
[aj] *Instituto de Fisica de Cantabria (CSIC-UC), Avd. de los Castros s/n, 39005 Santander, Spain*
[ak] *IFIC (UVEG/CSIC), Edificio Institutos de Investigación Apartado de Correos 22085 E-46071 Valencia, Spain*
[al] *University of Florida, Department of Physics, P.O. Box 118440, Gainesville, FL 32611, USA*
[am] *J. Stefan Institute, Faculty of Mathematics and Physics, University of Ljubljana, 1000 Ljubljana, Slovenia*
[an] *Peking University, Department of Technical Physics, Beijing 100871, China*

E-mail: benjamin.schwenker@phys.uni-goettingen.de

PoS(VERTEX2018)006

The construction of the new accelerator at the Super Flavor Factory in Tsukuba, Japan, has been finalized and the commissioning of its detector (Belle II) has started. This new e^+e^- machine (SuperKEKB) will deliver an instantaneous luminosity of 8×10^{35} cm^{-2}s^{-1}, which is 40 times higher than the world record set by KEKB. In order to be able to fully exploit the increased number of events and provide high precision measurements of the decay vertex of the B meson systems in such a harsh environment, the Belle II detector will include a new 6 layer silicon vertex detector. Close to the beam pipe, 2 pixel and 4 double-sided strip detector layers will be installed. During its first data taking period in 2018, the inner volume of the Belle II detector was only partially equipped with the final vertex detector technologies. The remaining volume was covered with dedicated radiation monitors, collectively called BEAST II, in order to investigate the particle and synchrotron radiation backgrounds near the interaction point. In this note, the milestones of the commissioning of the Belle II vertex detector and BEAST II are reviewed and the detector performance and selected background measurements will be presented.

The 27th International Workshop on Vertex Detectors - VERTEX2018
22-26 October 2018
MGM Beach Resorts, Muttukadu, Chennai, India

*Speaker.

1. Introduction

The SuperKEKB [1] asymmetric (4 GeV e^+, 7 GeV e^-) collider is an upgrade of the KEKB machine that will provide the Belle II experiment [2] an unprecedented instantaneous luminosity of 8×10^{35} cm^{-2}s^{-1}. The Belle II experiment aims to collect an integrated luminosity of about 50 ab^{-1} on the $\Upsilon(4S)$ resonance in ten years of operation. The increased statistics will allow to search for physics beyond the Standard Model in the heavy quark and lepton sectors.

The increase in luminosity is achieved on the one hand by roughly doubling the beam currents compared to the previous accelerator KEKB, on the other hand by a novel nano-beam scheme [3] which requires a beam size of order 10 μm $\times$ 60 nm at the interaction point and an increased crossing angle of the beams. The implementation of the nano-beam scheme requires extremely small emittances that can only be achieved by raising the energy of the low energy ring. This in turn implies a reduced center-of-mass boost compared to the previous B-factory experiments. In order to compensate the reduced spatial separation of the B-decay vertices, the new Belle II vertex detector (VXD) provides high-resolution measurements of charged particle tracks in the high radiation environment close to the collision region.

2. Design of the Belle II vertex detector

The Belle II vertex detector, shown in Fig. 1, is the innermost tracking detector of the Belle II experiment. It is made of six concentric barrel layers with mean radii of 14, 22, 39, 80, 104 and 135 mm centered around the beam axis. The inner two layers are equipped with 75 μm thick fully depleted p-channel FET (DEPFET [4]) sensors (PXD). The outer four layers are 300-320 μm thick double sided silicon strip sensors (SVD). The forward ring of three outermost SVD layers is formed by slanted sensors to economize material budget on the forward edge of acceptance. The six VXD layers hermetically cover the angle range $17^\circ < \theta < 150^\circ$ where θ is the angle measured from the interaction point with respect to the z axis. On the outside, the VXD is enveloped by another tracking detector, the Central Drift Chamber (CDC).

2.1 Design of the PXD detector

The PXD consists of 8 ladders in the innermost layer and 12 ladders in the second layer. The ladder is made up of two half-ladders of monolithic silicon, which are glued pairwise to form a self supporting structure. A main requirement for the PXD design was to minimize the material budget as much as possible in order to reduce multiple scattering of impinging particles. Concerning this matter, an advantage of DEPFET sensors is that they can be built very thin due to the internal signal amplification and the very low intrinsic noise of the device. The sensitive part of the half-ladder has a thickness of just 75 μm. The thinning technology uses anisotropic etching on bonded wafers to create a thin, fully self supporting sensor, where no external structures are needed. The stiffness is provided by a thick (525 μm) silicon rim around the sensor, where the auxiliary ASICs are directly bonded to. The material budget of the silicon rim is reduced by etching grooves into it. Furthermore, many parts of the readout electronics are mounted outside of the detector acceptance.

A pixel matrix of 250$\times$768 pixels is operated using a rolling-shutter architecture with 20 μs integration time. The gate and clear lines of the pixels, placed on the same matrix row, are con-

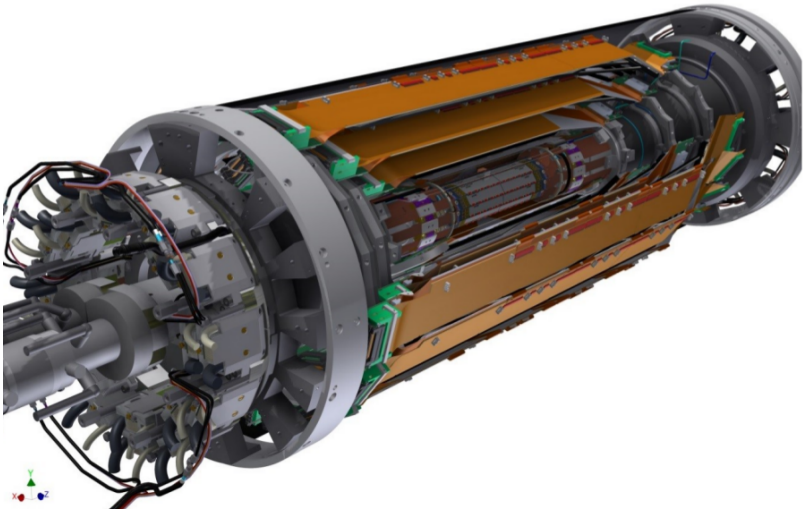

Figure 1: Belle II vertex detector layout

nected to a control chip (SwitcherB), which is responsible for selecting subsequent rows. An entire column of pixels is read out by a current receiver ASIC (DCDB or Drain Current Digitizer [5]). The data from the DCDB is further transmitted to the Data Handling Processor (DHP) [6], the third ASIC on the half-ladder, which performs pedestal subtraction, common mode correction and hit finding. Expected occupancy is 1 % (innermost layer) and trigger rate is 30 kHz at full luminosity. The DEPFET sensors and readout ASICs are designed to sustain an expected total ionizing dose of 20 Mrad for 10 years Belle II operation. In order to guarantee that the hit finder inside the DHP can process all data, the PXD hit occupancy must be below 3 %.

2.2 Design of the SVD detector

The SVD [7] consists of ladders that are basically arrays of double sided silicon strip sensors (DSSD). Layers 3,4,5 and 6 have 7, 10, 12 and 16 ladders. Each DSSD is either rectangular or trapezoidal having 300-320 μm thickness with n-type bulk whose one side is doped by acceptor (called strips) and the other side is doped by donor, with strips being perpendicular to the former. The acceptor implanted side, called p or U side, having longer strips parallel to the length of the sensor, measure the $r-\phi$ coordinate. The donor implanted (n or V side) shorter strips measure the z coordinate. The sensors have a readout pitch varying between 50-75 μm in the $r-\phi$ direction and 160-240 μm along the z axis. To improve the spatial resolution, one floating strip is implemented between two readout strips.

The SVD strips are AC coupled to the APV25 [8] low noise front-end readout chip, originally developed for the CMS strip detector readout system. With 50 ns shaping time and 6 samples per readout, SVD allows precise timing at the level of nanoseconds and is useful to seperate signal from background hits. The APV25 chips on the sensors within the tracking acceptance are thinned down to 100 μm to reduce material. The sensors are equipped with charge injection capability for precise charge response calibration. At full luminosity, the expected dose on the innermost SVD layer is 100 krad/yr and the average occupancy is 1.3 %. SVD sensors and chips are radiation hard

for total ionizing dose of 10 Mrad, ten times more than the expected dose in ten years. For optimal tracking performance, the SVD occupancy should be below 3 %.

3. VXD operation in Phase 2

The commissioning of the Belle II experiment is split in three phases. In Phase 1, before the Belle II roll-in, studies of the single beam backgrounds in the interaction region were conducted in 2016 [9]. In the next step, Phase 2, the Belle II detector was running from February to mid July 2018 with the final focusing magnet system already in place. The setup of the Phase 2 VXD is shown in Fig. 2. The six VXD layers have the geometry of the full VXD, except they comprise only a single ladder per layer in the horizontal plane. The remaining volume was occupied by the BEAST II VXD detectors: a hybrid silicon pixel detector with FE-I4 front end (FANGS [10]), plastic scintillator with SiPM readout (CLAWS [11]) and double sided ladders with active CMOS pixel sensors (PLUME [12]). Very close to the PXD and the innermost SVD layer, diamond sensors were installed for ionizing dose monitoring in the interaction region. The main goals of the Phase 2 VXD were commissioning of the final interaction region, measurement of beam background for safe installation of the full VXD in Phase 3 and acquisition of first collision data. At the end of Phase 2, the complete Phase 2 VXD volume including the beam pipe will be disassembled and replaced with the final beam pipe and VXD for Belle II.

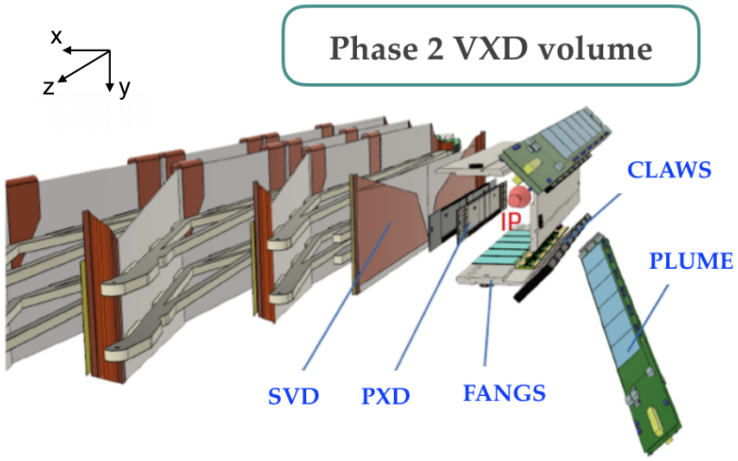

Figure 2: Phase 2 VXD layout with 4 layers of SVD, 2 layers of PXD and additional sensors for background monitoring in the VXD volume

The four SVD ladders and two PXD ladders for Phase 2 were attached to the beam pipe and integrated with the rest of Belle II in between September and November 2017. The PXD and SVD ladders installed into Phase 2 are B grade ladders from the final sensor production which were previously tested in a combined PXD and SVD test beam at DESY in April 2016. Due to problems with the gluing process, the ladders of the Phase 2 PXD consisted of mechanically disjoint pairs of half-ladders. The Phase 2 VXD has been operated for the first time in a cosmic run from February to March 2018. Phase 2 running started with the injection of first beams beginning of April and

all BEAST II detectors were always running since providing particle rates from beam background to the accelerator control room. Storage of single electron and positron beams in SuperKEKB was achieved in April and first collisions were recorded on the 26th of April. Phase 2 running was stopped on schedule on the 18th of July.

To protect the front-end electronics and sensors from the effects of beam incidents a "stable beam" interlock has been implemented. Until beams were declared stable by the accelerator control room using particle rates from BEAST II detectors, mainly Diamonds and CLAWS, the PXD and SVD sensors were not depleted and only the front-end chips were powered and configured. This avoids that a high charge deposition in the double-sided strip sensors causes a sudden drop in the voltage across the silicon bulk, potentially causing a breakdown of the AC capacitor integrated on the implanted sensor strips. Once stable beams were declared, after additional checks of the beam conditions, the high voltage for depleting the sensors was ramped up and a new run could be started. It was found in dedicated tests that the PXD can be operated and read-out without harm during the injection of new beams.

4. Offline performance examples

All four PXD sensors were operated during Phase 2 and three out of four sensors showed excellent performance with low noise and a small fraction of dead pixels (<3 %). These dead pixels are mostly known shorts in drain lines of the pixel matrix on B grade sensors. On the fourth sensor one quarter of the pixel matrix could not be read-out due to a bad mechanical connection of an optical fiber at the PXD dock box. The signal to noise ratio distribution for clusters is shown in Fig. 3 for a physics run near the end of Phase 2. The noise of each cluster is computed as the sum in quadrature of the noise of the single pixels, while the cluster charge is the sum of the charges of all pixels forming the cluster. The average single pixel noise varies from 0.69 to 0.71 ADU between the four sensors. A hit threshold of 5 ADU was applied in the front-end electronics and the highest charge in the cluster was required to be above 7 ADU. The clusters are not required to be matched to a charged track and the distribution is expected to contain clusters from background radiation accumulated during the 20 μs integration time of the PXD. The signal to noise ratio extracted from a Landau fit to the distributions is just above 50 for all four sensors. The pixels sensors in the innermost layer have a second peak originating from low energy single pixel clusters. A preliminary energy calibration of the PXD shows that these peaks are in the range of 7-10 keV. The origin of this low energy radiation component is still under investigation, but simulations of the synchrotron radiation backgrounds can reproduce peaks in the range of 7-10 keV in qualitative agreement with data.

One of the most important aspects of the detector performance is the efficiency. Figure 4 shows the efficiency at which for a reconstructed track a hit can be found on the four different PXD sensors. The hit efficiency is reported for randomly selected physics runs near the end of Phase 2. Reconstructed tracks with a momentum $p > 4$ GeV and at least hits in three SVD layers are extrapolated into the Phase 2 PXD. Tracks extrapolated into the vicinity of dead pixels are excluded. The tight track selection requirements in combination with the small geometrical acceptance of the Phase 2 PXD setup leads to large statistical uncertainties on the efficiency for runs with short duration. The average efficiency over all runs is better than 97 % for all four sensors.

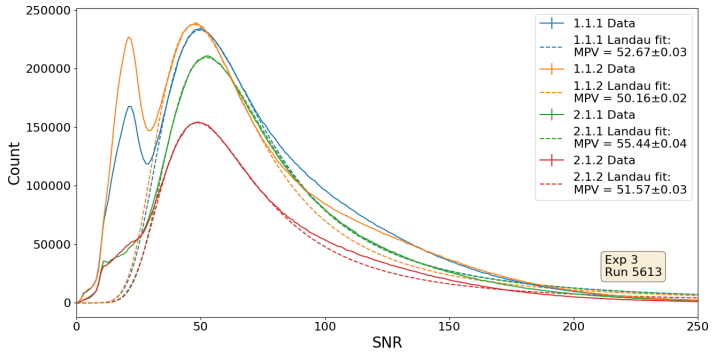

Figure 3: Signal to noise ratio for all four pixel sensors in the Phase 2 PXD.

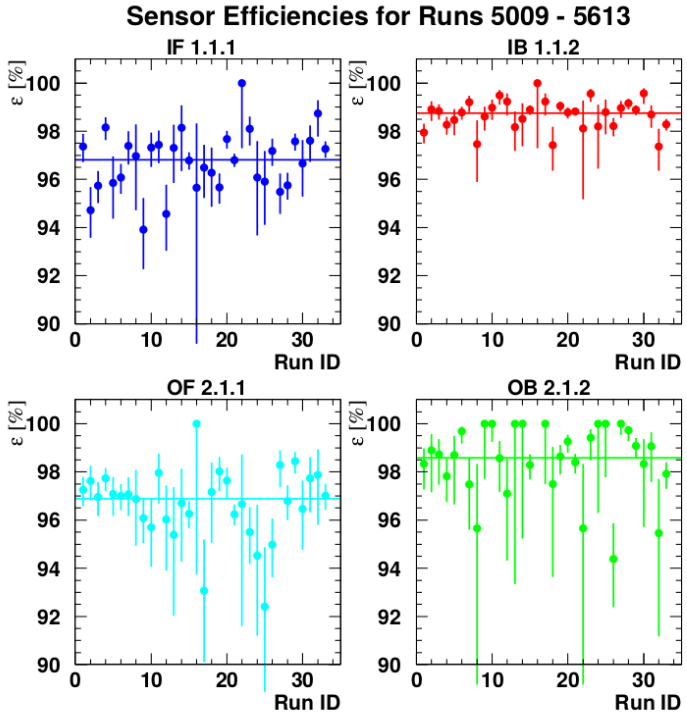

Figure 4: Hit efficiency of all four PXD sensors for randomly selected runs near the end of Phase 2.

The signal to noise ratio distribution for SVD clusters related to tracks is shown in Fig. 5. The signal to noise ratio is computed separately for U/P and V/N clusters. The noise of each cluster is computed as the sum in quadrature of the noise of the single strips, while the cluster charge is the sum of the charges of the strips forming the cluster. The typical signal to noise ratio measured is about 30 for V/N side, and about 20 on U/P side with higher noise, due to the longer strips and larger capacitance load to the pre-amplifier. The cluster time distribution for clusters related to tracks in Fig. 6. resolves the filling pattern of the SuperKEKB accelerator in Phase 2 with different bunches. The two main peaks in the middle correspond to clusters created by tracks belonging to

the bunch crossings that has happened in the APV25 clock period expected from the trigger signal. The width of each peak shows that the SVD hit timing resolution, although at a very early stage of calibration, is well below 10 ns, as expected.

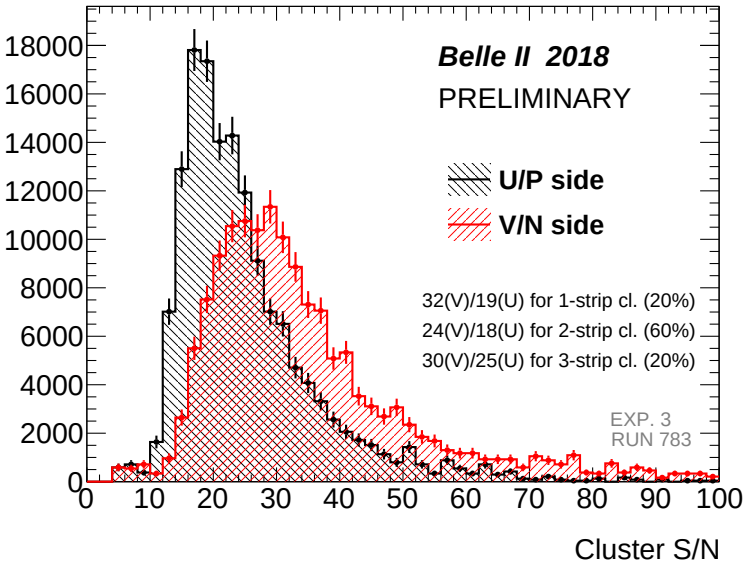

Figure 5: Signal to noise ratio for clusters related to tracks traversing large rectangular SVD sensors.

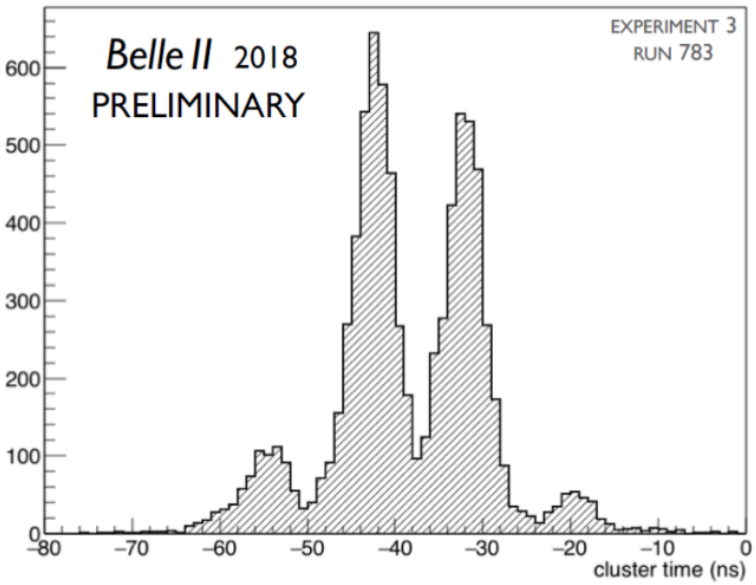

Figure 6: Reconstructed time for V-clusters related to tracks traversing large rectangular SVD sensors.

5. Background studies in Phase 2

With the increased luminosity of SuperKEKB, the beam background is expected to grow sig-

nificantly with respect to KEKB, leading, among other effects, to possible damage of detector components and suppression of signal events. The Phase 2 experiment provided a unique opportunity to measure beam backgrounds in the interaction region before the installation of the final Belle II vertex detector. The purpose of the Phase 2 operation, together with the commissioning of SuperKEKB in its final configuration, is to verify that the level of backgrounds in the interaction region are compatible with the expectations and safe for the installation of the complete vertex detector.

Background sources in Belle II can be separated in single beam backgrounds and luminosity dependent backgrounds. Single beam backgrounds, like the Touschek effect, beam-gas scattering and synchrotron radiation can be split further into contributions from the high energy electron ring (HER) and the low energy positron ring (LER). The term "luminosity-dependent processes" groups together all physics processes that are initiated by the collision of the electron and the positron beam. This comprises physics processes as well as processes that contribute to the background of the Belle II detector, like radiative Bhabha scattering and two-photon processes. In Phase 3 at full luminosity, the background occupancy in the innermost SVD layer is expected to be dominated by the luminosity dependent term (83 %) while the contribution from single beams is 15 % for LER and 2 % for HER. In Phase 2, the background in the vertex detector volume is expected to be dominated instead by single beam contributions: LER 80 %, HER 2 %, luminosity 18 %.

During the last two weeks of Phase 2, dedicated single beam studies for backgrounds from LER and HER rings have been conducted using the same beam optics that will be applied for the start of Phase 3. A series of runs with different vertical beam size σ_y were taken and the background occupancy in the PXD and SVD sensors have been recorded at 1 Hz to follow dynamic changes in beam current or the residual pressure in the beam pipe. Touschek and beam-gas contributions were evaluated fitting the data with a two-parameters function [9] that describes their dependence from beam parameters:

$$O = T\frac{I^2}{\sigma_y n_b} + BZ_{\text{eff}}^2 Ip$$

where O is a measured particle rate, T is the parameter for the Touschek component and B is the parameter for the beam-gas component. The other variables are the number of bunches n_b, the effective nuclear charge Z_{eff} of residual gas atoms in the beam pipe, the beam current I and the residual gas pressure p. It can be seen in Fig. 7 that this function well represents the data of the LER studies for runs with different beam sizes σ_y. The predicted contributions B and T were extracted from a series of run dependent MC simulations which take into account the beam optics and collimator positions in the SuperKEKB accelerator. The ratios between data and MC for the parameters B and T are given in Tab. 1. The agreement for LER studies is reasonable but a huge discrepancy is found for HER studies. The pattern is very similar in PXD and SVD. The simulation appears to underpredict the HER backgrounds in the VXD by two orders of magnitude and the observed HER and LER backgrounds are much more similar than predicted. Rescaling the beam background predictions for full luminosity Phase 3 runs, using the extracted ratios Data/MC ratios from Phase 2, gives a too high occupancy in PXD and SVD and requires a reduction of backgrounds by a factor of 10. Recent work on improving the beam pipe shape in the simulation

and adding a beam-gas bremsstrahlung component increases the predicted HER backgrounds by an order of magnitude.

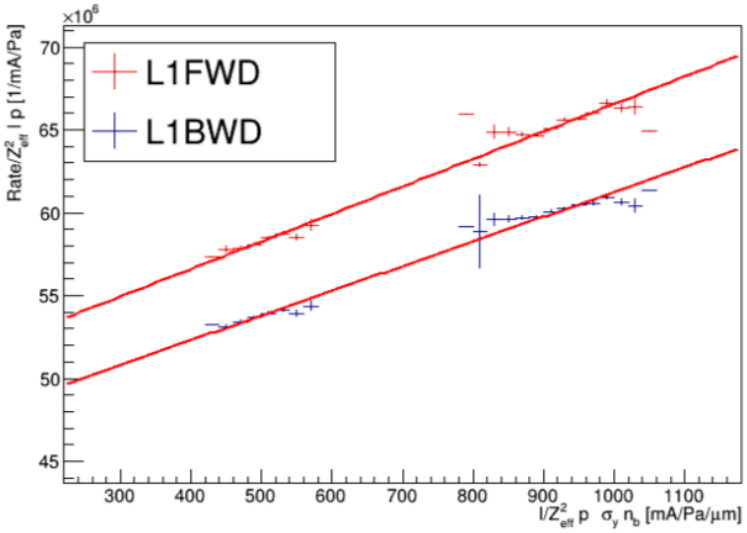

Figure 7: Data of beam size study for LER with Touschek and beam-gas components. The measured observable O is the rate of multi-pixel clusters in innermost PXD layer.

	Rate Data/MC Layer 1 (PXD) min-max	**Rate Data/MC Layer 3 (SVD)** min-max
HER Beam-gas	480-510	270-610
HER Touschek	360-370	260-350
LER Beam-gas	15-16	11-13
LER Touschek	2.4-2.5	2.3-2.9

Table 1: Ratios of measured to predicted contributions for the Touschek and beam-gas background components in Phase 2.

6. Summary

The Belle II experiment has completed the Phase 2, with a subset of the final Belle II vertex detector comprising six layers with a single ladder per layer. First physics collisions have been successfully recorded at the end of April 2018 and and a total luminosity of 500 pb^{-1} have been collected for physics studies.

All BEAST II detectors were operational and provided valuable online feedback for machine commissioning and safe operation of Belle II during Phase 2. SVD key operation features like signal to noise ratio and hit time resolution are within or exceeding TDR expectation. PXD demonstrated stable operation of four half-ladders with low noise and an excellent signal to noise ratio.

Background from soft photons in the energy range 7-10 keV was observed in the PXD, FANGS and radio-chromic foils and is in qualitative agreement with simulation of synchrotron radiation.

Single beam background from the low energy ring is in reasonable agreement with MC prediction within a factor 3-10 for SVD and PXD while the the background from the high energy ring is underpredicted. The observed HER and LER background rates are much more similar than predicted and the overall sum of backgrounds is about 10 times too high for efficient operation of the VXD at full luminosity. Ways for mitigating the backgrounds by tuning the accelerator and installing additional collimators are currently under study. The Phase 2 run confirmed that the full VXD could be safely installed for the early part of Phase 3 in March 2019.

7. Acknowledgments

This work is supported by MSCA-RISE project JENNIFER (EU grant n.644294); MEXT, WPI, and JSPS (Japan); ARC (Australia); BMWFW (Austria); MSMT (Czechia); AIDA-2020, BMBF (Germany); DAE and DST (India); INFN (Italy); NRF-2016K1A3A7A09005605 and RSRI (Korea) and MNiSW (Poland); and MINECO grant FPA2015- 71292-C2-1-P (Spain). Many thanks to the Belle II Beam Background group, Belle II Commissioning Group (BCG) and SuperKEKB group.

References

[1] Y. Ohnishi *et al.*, *Accelerator design at SuperKEKB*, PTEP 2013, 03A011, DOI: 10.1093/ptep/pts083

[2] T. Abe *et al.*, *Belle II Technical Design Report*, 2010

[3] M. Baszczyk *et al.*, *SuperB Technical Design Report*, arXiv:1306.5655 [physics.ins-det]

[4] J. Kemmer and G. Lutz, *New detector concepts*, Nucl.Instrum.Meth. A 253 no. 3, (1987)

[5] I. Peric, P. Fischer and T. H. H. Nguyen, *DCDB and SWITCHERB, the readout ASICS for Belle II DEPFET pixel detector*, IEEE Nucl. Sci. Symp. Conf. Rec. 2011 (2011) 1536

[6] M. Lemarenko, T. Hemperek, H. Krüger, M. Koch, F. Lütticke, C. Marinas and N. Wermes, *Test results of the data handling processor for the DEPFET pixel vertex detector*, JINST 8, 2013

[7] K. Adamczyk *et al.*, *The silicon vertex detector of the Belle II experiment*, Nucl. Instrum. Meth. A 824, 2016

[8] M. French *et al.*, *Design and results from the APV25, a deep sub-micron CMOS front-end chip for the CMS tracker*, Nucl. Instrum. Meth. A 466, 2001

[9] P. M. Lewis *et al.*, *First Measurements of Beam Backgrounds at SuperKEKB*, Nucl. Instrum. Meth. A 914, 2019

[10] P. Ahlburg, *Development of a FE-I4-based module for radiation monitoring with BEAST II during the commissioning phase of the Belle II detector*, MSc Thesis, University of Bonn, https://www.hep1.physik.uni-bonn.de/results/data/internal/patrick-ahlburg

[11] D. Heuchel, *CLAWS in BEAST Phase II: Investigation of the Beam Background in the Commissioning of SuperKEKB*, MSc Thesis, TU München, Germany, 2018 [MPP-2018-8], https://publications.mppmu.mpg.de/2018/MPP-2018-8/FullText.pdf

[12] J. Baudot, *BEAST results on SuperKEKB beam induced background with special emphasis on the PLUME pixelated system*, International Workshop on Semiconductor Pixel Detectors for Particles and Imaging (PIXEL2018), https://indico.cern.ch/event/669866/contributions/3242084